PHYSICAL REVIEW B **79**, 180408(R) (2009)

Electric polarization induced by transverse magnetic field in the anisotropy-controlled conical helimagnet $Ba_2(Mg_{1-x}Zn_x)_2Fe_{12}O_{22}$

S. Ishiwata,[1,*] Y. Taguchi,[1] Y. Tokunaga,[2] H. Murakawa,[3] Y. Onose,[3,4] and Y. Tokura[1,3,4]
[1]*Cross-correlated Materials Research Group (CMRG), Advanced Science Institute, RIKEN, Wako 351-0198, Japan*
[2]*Multiferroics Project, ERATO, JST, c/o RIKEN, Wako 351-0198, Japan*
[3]*Multiferroics Project, ERATO, JST, c/o Department of Applied Physics, University of Tokyo, Hongo, Tokyo 113-8656, Japan*
[4]*Department of Applied Physics, University of Tokyo, Hongo, Tokyo 113-8656, Japan*
(Received 22 January 2009; revised manuscript received 13 April 2009; published 20 May 2009)

Microscopic origin of magnetic-field (B) induced electric polarization (P) potentially up to near room temperature has been investigated for helimagnets $Ba_2(Mg_{1-x}Zn_x)_2Fe_{12}O_{22}$ with controlled magnetic anisotropy by revealing B- and x-dependent changes of magnetoelectric responses. As Zn concentration (x) increases, the B-induced P rapidly diminishes, accompanying the change in the magnetic-easy surface from conical to planar. Possible spin structures are proposed to explain the observed B dependence of P in terms of the spin-current model. The results indicate the important role of magnetic anisotropy in the B-induced ferroelectric state of this class of helimagnets.

DOI: 10.1103/PhysRevB.79.180408 PACS number(s): 75.50.Dd, 75.25.+z, 75.30.Gw, 75.80.+q

The strong coupling between magnetization and electric polarization in a solid is currently of great interest in light of the off-diagonal response against external fields. The discovery of a gigantic magnetoelectric (ME) effect in $TbMnO_3$ and the subsequent studies have established the fact that a spiral spin order and the accompanied lattice distortion cause symmetry breaking and produce a ferroelectric polarization.[1–6]

Considering the spin current, Katsura *et al.*[7] derived the microscopic relation between the electric polarization vector $\boldsymbol{p}$ and the noncollinearly aligned, neighboring spins $\boldsymbol{s}_i$ and $\boldsymbol{s}_j$, which is given by $\boldsymbol{p}=A\boldsymbol{e}_{i,j}\times(\boldsymbol{s}_i\times\boldsymbol{s}_j)$, where $\boldsymbol{e}_{i,j}$ denotes the unit vector connecting the spins, $\boldsymbol{s}_i$ and $\boldsymbol{s}_j$. A is a constant which depends mainly on the exchange interaction and the spin-orbit interaction.[7,8] This relation can be considered as an inverse effect of the Dzyaloshinski-Moriya interaction, when the inevitable lattice distortion is taken into account.[9,10] According to this relation, cycloidal and transverse conical helimagnets, the screw axis of which is perpendicular to the propagation vector $\boldsymbol{k}_0(\boldsymbol{e}_{i,j}=\boldsymbol{k}_0/|\boldsymbol{k}_0|)$, are allowed to have a ferroelectric polarization $\boldsymbol{P}=\Sigma_{i,j}A\boldsymbol{k}_0\times(\boldsymbol{S}_i\times\boldsymbol{S}_j)/|\boldsymbol{k}_0|$. As for proper screw and longitudinal conical helimagnets, the screw axis of which is parallel to $\boldsymbol{k}_0$, the transverse conical spin structure can be stabilized to yield a finite $\boldsymbol{P}$ with the application of magnetic field ($\boldsymbol{B}$) nonparallel to $\boldsymbol{k}_0$, as demonstrated in $ZnCr_2Se_4$ (Ref. 11) and $Ba_2Mg_2Fe_{12}O_{22}$.[12]

While the rich magnetic phase diagrams of the spin-frustrated materials allow us to explore a gigantic ME response, the available temperature or field ranges are far from what is necessary for practical applications. Y-type hexaferrites have great potential to overcome such limitations.[13] $Ba_{0.5}Sr_{1.5}Zn_2Fe_{12}O_{22}$ has an exceptionally high ordering temperature of about 320 K for a proper-screw phase and shows magnetic phase transitions upon application of $\boldsymbol{B}$ perpendicular to the propagation vector $\boldsymbol{k}_0(\|[001])$.[14] Kimura *et al.*[13] found that one of the B-induced phases has a ferroelectric polarization $\boldsymbol{P}$ perpendicular to both $\boldsymbol{k}_0$ and $\boldsymbol{B}$. However, the emergence of P requires application of B larger than 0.25 T, and the relation has not been very clear between $\boldsymbol{P}$ and either the fanlike spin structure proposed for the ferroelectric phase[14] or the helimagnetic structure at zero field.

Recently, it was found that an isostructural helimagnet $Ba_2Mg_2Fe_{12}O_{22}$ has ferroelectric phases in the very low-field region, named FE1 and FE2, additionally to the phase at around 1 T, named FE3 phase.[12,15] As shown in Fig. 1(a), magnetically ordered states can be described by the alternate stacking of the L block with the large magnetic moments and the S block with the smaller magnetic moments (the spins are aligned ferrimagnetically in each block). This material undergoes transitions from a collinear ferrimagnetic phase to a proper-screw phase [Fig. 1(b)] at 195 K and to a longitudinal conical phase [Fig. 1(c)] at around 50 K. The presence of the uniform magnetization associated with the conical spin state makes the Zeeman energy in a small magnetic field more important than the anisotropy energy and, therefore, enables the low-field (as weak as 30 mT) control of spin helix and, hence, the $\boldsymbol{P}$ vector.[12,16]

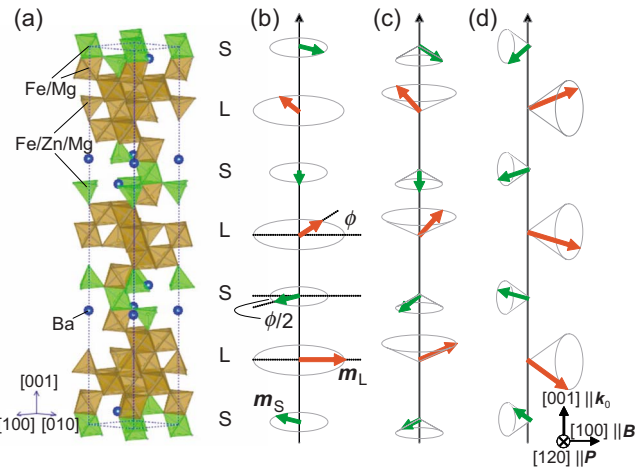

FIG. 1. (Color online) (a) Schematic crystal structure of $Ba_2(Mg_{1-x}Zn_x)_2Fe_{12}O_{22}$. (b)–(d) Illustrations of helicoidal magnetic structures consisting of alternate stacks of the L blocks (having the larger magnetic moments) and S blocks (having the smaller magnetic moments) with a propagation vector k_0 along the c axis; (b) proper screw, (c) longitudinal conical, and (d) transverse conical spin structures.

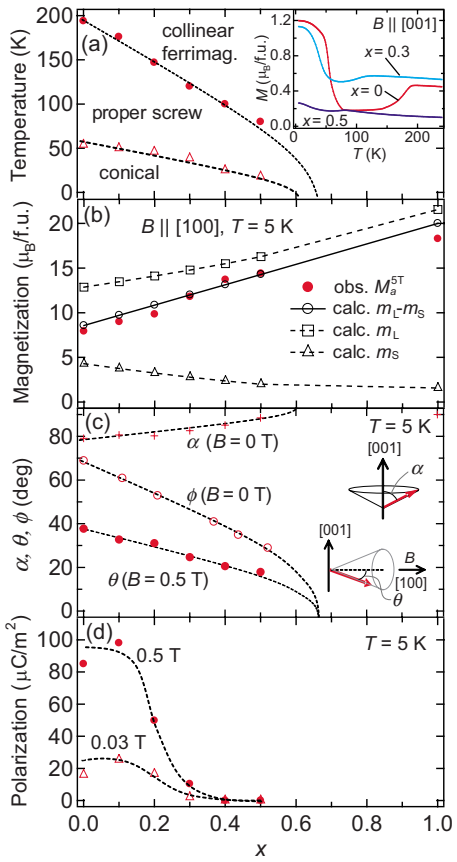

FIG. 2. (Color online) Zn-doping (x) dependence of various physical properties of $Ba_2(Mg_{1-x}Zn_x)_2Fe_{12}O_{22}$ single crystals. (a) T-x magnetic phase diagram (the inset shows representative M-T curves measured under a magnetic field ($\boldsymbol{B}$) of 0.01 T along [001]), (b) saturation magnetization $M_a^{5\ \mathrm{T}}$ measured with $\boldsymbol{B}$ of 5 T along [100] and the calculated values of m_L, m_S, and m_L-m_S, (c) cone angles of the longitudinal conical (α) and the transverse conical (θ) spin structures, the turn angle (ϕ) reproduced from Ref. 17, and (d) electric polarizations (P) at 0.03 and 0.5 T. P at 0.03 T was measured after sweeping $\boldsymbol{B}$ across zero field.

Despite these advantages of the Y-type hexaferrites, there remain uncertainties regarding the relation between the ferroelectricity and the magnetic properties, especially the magnetic anisotropy. To solve the problem, a solid solution $Ba_2(Mg_{1-x}Zn_x)_2Fe_{12}O_{22}$ was prepared; the series shows a systematic change in the magnetic ground state[17] from the collinear ferrimagnetic state for $x=1$ to the conical state for $x=0$ [see also Fig. 2(a)]. This change reflects the difference of the preferential sites between Mg and Zn, leading to the different distribution of Fe^{3+} ions over tetrahedral and octahedral sites. Actually, neutron-diffraction studies have revealed that Mg^{2+} ions prefer octahedral sites, whereas the Zn^{2+} ions occupy only tetrahedral sites.[17–19] Depending on the magnetocrystalline anisotropy at each crystallographic site, the magnetic-easy direction of the Y-type hexaferrites can be uniaxial, planar, or even conical.[20] In this Rapid Communication, we present a systematic study of the ME properties of $Ba_2(Mg_{1-x}Zn_x)_2Fe_{12}O_{22}$ to provide insight into the relation between conical spin structures and $\boldsymbol{P}$. We have found that the presence of the magnetic-easy conical surface plays an important role for the ferroelectricity associated with transverse conical spin structures in the helimagnetic hexaferrites.

Single-crystalline samples of $Ba_2(Mg_{1-x}Zn_x)_2Fe_{12}O_{22}$ were grown by a flux method as described in Ref. 17. For the measurements of $\boldsymbol{P}$, gold electrodes were deposited on both the end faces of the rectangularly shaped crystals. The poling procedure can be found in Ref. 12. The displacement current was integrated as a function of time to obtain the $\boldsymbol{P}$ value. The magnetic properties were measured with a superconducting quantum interference device (SQUID) magnetometer.

Figure 2 summarizes the magnetic and electronic properties of $Ba_2(Mg_{1-x}Zn_x)_2Fe_{12}O_{22}$ as a function of the Zn concentration (x). The transition temperatures from a collinear ferrimagnetic to a proper screw and to a longitudinal conical phase were determined from the temperature-dependent magnetization measured upon decrease in temperature [Fig. 2(a)]. The essentially same phase diagram apart from the conical phase has been reported by Momozawa *et al.*[17] The open squares and triangles connected with dotted lines in Fig. 2(b) represent the moments for the L block (m_L) and the S block (m_S), respectively, which were calculated with the assumptions that each $Fe^{3+}(S=5/2)$ ion has the magnetic moment of $5\mu_B$ and that the obtained solid solutions have the same x dependence of cation distribution as those reported in Ref. 17. A systematic change in the saturation magnetization along [100]($M_a^{5\ \mathrm{T}}$) with the increase in x, which is in good agreement with thus calculated value of m_L-m_S, ensures successful syntheses of the single-crystalline solid solution $Ba_2(Mg_{1-x}Zn_x)_2Fe_{12}O_{22}$. All the compounds are in the collinear ferrimagnetic state at 5 T [Figs. 3(i)–3(l)].

In addition to the magnetic transition temperatures [Fig. 2(a)] and $M_a^{5\ \mathrm{T}}$ [Fig. 2(b)], Zn doping systematically changes the cone angles at zero field (α) and at $B=0.5$ T (θ) parallel to [100] at 5 K, as shown in Fig. 2(c). α was estimated from the remnant magnetization along [001] ($\cos\alpha=M_c^{0\ \mathrm{T}}/M_c^{5\ \mathrm{T}}$) and θ was estimated from the ratio of the magnetization along [100] ($\cos\theta=M_a^{0.5\ \mathrm{T}}/M_a^{5\ \mathrm{T}}$).[21] The turn angle ϕ between the adjacent L (or S) blocks at 5 K, taken from the Ref. 17, is also appended for reference [Fig. 2(c)]. The x-dependent changes in α and θ reflect the variation in the magnetic anisotropy; the increase in the Zn concentration stabilizes the easy-plane anisotropy and consequently destabilizes the longitudinal conical spin structure. Since the single-ion anisotropy is expected to be different depending on the local symmetry, the change in the magnetic anisotropy in $Ba_2(Mg_{1-x}Zn_x)_2Fe_{12}O_{22}$ as a function of x can be ascribed to the difference in the preferential site for Mg and Zn and resultant variation in the Fe occupation.

The ME phase diagrams [Figs. 3(i)–3(l)] of $Ba_2(Mg_{1-x}Zn_x)_2Fe_{12}O_{22}$ were determined by magnetization curves measured on increasing B along [100], as shown in Figs. 3(e)–3(h). The phase boundaries determined by the polarization measurements are also plotted. The FE3 phase at around 1 T exists robustly against the Zn doping. Thus, it is natural to assume that the magnetic structure of the FE3 phase is essentially similar to that of the ferroelectric phase having a commensurate propagation vector in $Ba_{0.5}Sr_{1.5}Zn_2Fe_{12}O_{22}$.

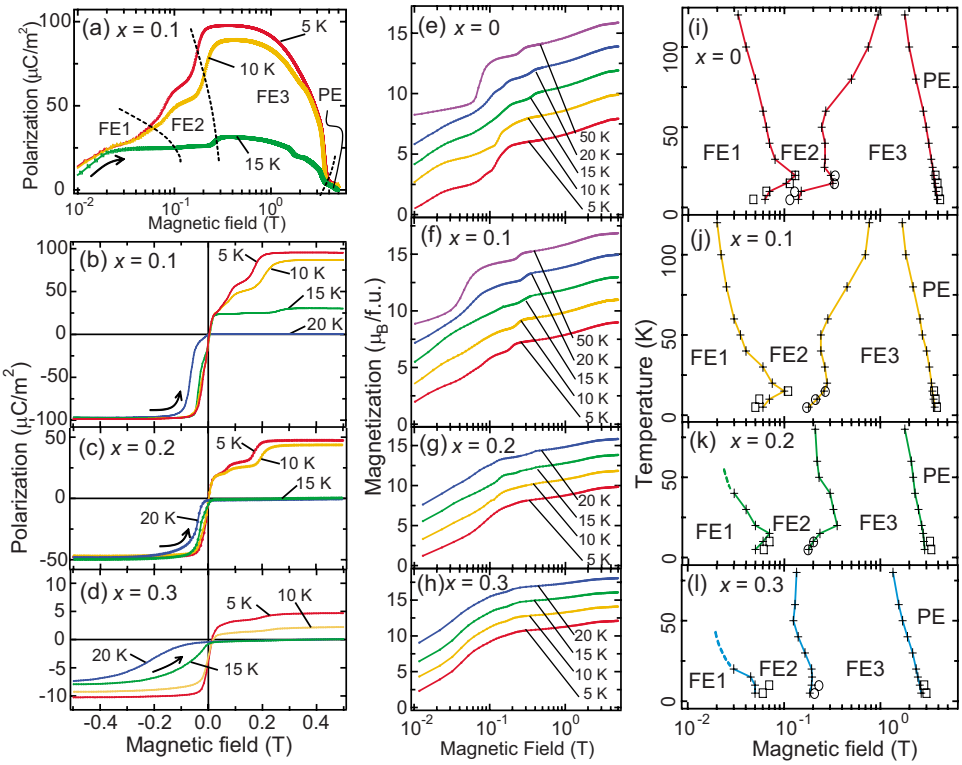

FIG. 3. (Color online) (a) Magnetic-field (B) dependence of electric polarization in $Ba_2(Mg_{0.9}Zn_{0.1})_2Fe_{12}O_{22}$ at 5, 10, and 15 K. The broken lines indicate phase boundaries. (b)–(d) Reversal and decay of electric polarization by a sweep of B along [100]. The data were collected on sweeping B from −1 to 5 T along [100] (the data are shown for $B \geq -0.5$ T). (e)–(h) Selected magnetization curves (for clarity, each magnetization curve except for at 5 K is shifted upward by $2\mu_B$/f.u. and (i)–(l) ME phase diagrams as a function of B along [100]. Cross marks and open symbols represent anomalies in the magnetization and polarization data, respectively. FE1–FE3 denote three ferroelectric phases and PE corresponds to a paraelectric phase having the collinear ferrimagnetic structure.

Figures 3(a) and 3(b) are representatives of the polarization curves measured with sweeping B from −0.5 to 5 T. As exemplified in Fig. 3(a) for the case of $x=0.1$, P increases in a stepwise manner as the phase changes as FE1 → FE2 → FE3 and then decreases with further increasing B in the FE3 phase. The asymmetry of the P-B curves for $x=0.1-0.3$ in Figs. 3(b)–3(d) reflects the strong hysteretic nature of the B-induced magnetic phase transitions; i.e., the FE3 phase widely prevails close to $B=0$ T in the negative B region, preventing a quantitative discussion for the magnitude of P in the FE1 phase. For $x=0.1$ [Fig. 3(b)], while P at −0.5 T remains almost the same with increasing temperature up to 20 K, its absolute value after sweeping B across the phase transitions drastically decreases when the temperature is elevated above 15 K. The significant decay of P upon sweeping B can be ascribed to the first-order nature of the transitions because it depends whether or not the spin helicity remains the same on traversing the first-order transition. Nevertheless, P appears to be conserved upon the B-induced phase transitions at 5 K, implying the presence of complex mechanisms such as the frozen domain-wall motion for the conservation of P. As x is increased [Figs. 3(c) and 3(d)] the polarization value at −0.5 T itself becomes smaller, and the polarization reversal tends to be possible only at lower temperatures.

For $x=0$ and 0.1, the behavior of the polarization as functions of field and temperature is very similar. As shown in Fig. 2(d), however, when the Zn concentration x increases, P at 0.03 (FE1) and 0.5 T (FE3) at 5 K show drastic changes near $x=0.3$ and vanish in the range where $x \geq 0.4$. Thus $x=0.4$ is the critical composition for the disappearance of ferroelectricity in $Ba_2(Mg_{1-x}Zn_x)_2Fe_{12}O_{22}$, which is likely due to the destabilization of the transverse conical state associated with the change in the magnetic anisotropy from conical to planar.

Next, we will discuss possible models for the FE3 phase. Figures 4(a)–4(d) show the B dependence of P for $Ba_2(Mg_{1-x}Zn_x)_2Fe_{12}O_{22}$ at 5 K and the calculated values based on the models (illustrated on the right side). Taking into account the neutron-diffraction studies for essentially the same phase in $Ba_{0.5}Sr_{1.5}Zn_2Fe_{12}O_{22}$,[14] the same commensurate propagation vector, $\boldsymbol{k}_0=\langle 003/2\rangle$ with two-time periodicity, is adopted for both models A and B. Although the model proposed by the neutron-diffraction studies is a fanlike spin structure with all spins lying on the c plane, we consider that some of the spins should be out of the c plane so that a finite $\boldsymbol{P}$ may appear along [120]. Thus, both models can be regarded as a kind of transverse conical spin structures with the two-time periodicity. Given that the exchange interaction is a dominant factor for the helimagnetic structure, it is reasonable to assume that all the ferroelectric phases (FE1–3) have a transverse conical spin structure and that the magnetic periodicity changes upon the change in the cone angle so as to minimize the loss of the exchange interaction energy. In the case of model A, the spins in the S blocks are slightly canted out of the c plane while the spins in the L blocks are lying on it. On the other hand, the spins in model B are constrained to lie on the longitudinal conical surface (drawn by the dotted lines) which are the magnetic-easy surface.

On the basis of the spin-current model, we derived the relations, $P \propto m_S m_L \sin^2\theta$ and $P \propto m_S m_L \cos\alpha(\sin^2\alpha - \cos^2\theta)^{1/2}$ for models A and B, respectively. Here, θ is estimated from the relation of $\theta=\arccos(M_a^B/M_a^{5\ \mathrm{T}})$. The plots in Figs. 4(a)–4(d) demonstrate that model B gives a better fit to the P-B curves than model A. This indicates the impor-

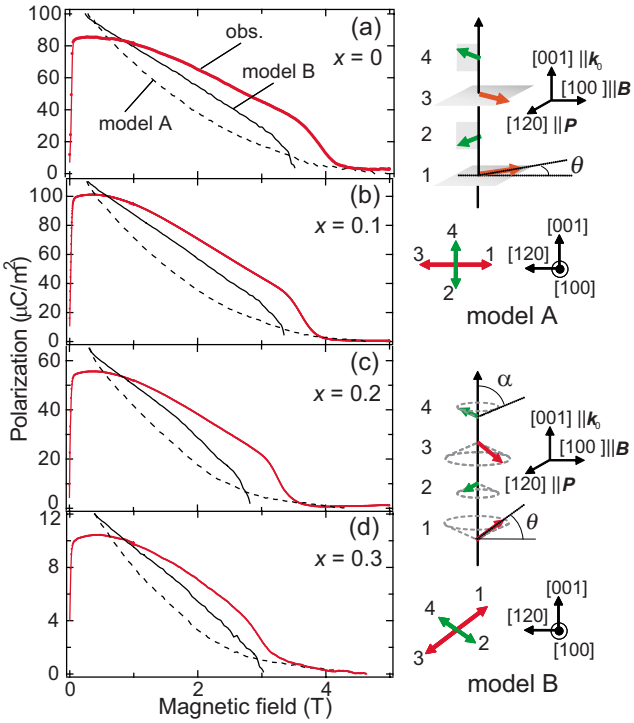

FIG. 4. (Color online) (a)–(d) Magnetic-field (applied along [100]) dependence of electric polarization of $Ba_2(Mg_{1-x}Zn_x)_2Fe_{12}O_{22}$ at 5 K. The data above and below 1 T were taken by increasing and decreasing the magnetic field, respectively. The solid and broken lines represent the calculated values, assuming models A and B, respectively. Schematic magnetic structures of models A and B are shown in the right side, together with their simplified illustrations viewed along the screw axis [100]. In model B, the angles which the L spin (S spin) makes with [100] and [001] are $\theta(\pi-\theta)$ and α or $\pi-\alpha$ (α or $\pi-\alpha$), respectively.

tance of the magnetic-easy conical surface for the B-induced transverse conical spin structure. The deviation between the model and the experimental data is expected to be reduced by considering the lattice degrees of freedom coupled to P, which is not involved in our models but is in reality very important.[22,23] The presence of the magnetic-easy conical surface in $Ba_2Mg_2Fe_{12}O_{22}$ is compatible with the experimental fact that the FE3 phase suddenly disappears when the direction of $\boldsymbol{B}$ is deviated from the c plane by more than 15° at 5 K,[12] which can be explained by a transition from the transverse conical to the longitudinal conical spin structure. To ascertain the validity of these models, neutron-diffraction measurements under magnetic fields are indispensable.

In summary, we have investigated the B-induced polarization of $Ba_2(Mg_{1-x}Zn_x)_2Fe_{12}O_{22}$ and discussed the relation between the magnetism and the ferroelectricity. The increase in Zn concentration results in destabilizing the longitudinal conical spin structure in zero field as well as the transverse conical spin structure in transverse magnetic fields and, hence, the ferroelectricity. The semiquantitative analyses based on the spin-current model have yielded a link between them, that is, a possible magnetic structure for the FE3 phase and the electric polarization. This work provided a comprehensive survey of the ME effect in the helimagnetic hexaferrites and showed a possibility of the improvement of the effect by controlling the magnetic anisotropy.

The authors thank T. Arima, N. Kida, S. Miyahara, and H. Katsura for useful discussions. This study was in part supported by Grant-in-Aid for Scientific Research on Priority Areas "Novel States of Matter Induced by Frustration" from the MEXT (Contract No. 20046017) and by Murata Science Foundation.

*ishiwata@riken.jp

[1] T. Kimura, T. Goto, H. Shintani, K. Ishizaka, T. Arima, and Y. Tokura, Nature (London) **426**, 55 (2003).
[2] M. Kenzelmann, A. B. Harris, S. Jonas, C. Broholm, J. Schefer, S. B. Kim, C. L. Zhang, S.-W. Cheong, O. P. Vajk, and J. W. Lynn, Phys. Rev. Lett. **95**, 087206 (2005).
[3] G. Lawes, A. B. Harris, T. Kimura, N. Rogado, R. J. Cava, A. Aharony, O. Entin-Wohlman, T. Yildirim, M. Kenzelmann, C. Broholm, and A. P. Ramirez, Phys. Rev. Lett. **95**, 087205 (2005).
[4] Y. Tokura, Science **312**, 1481 (2006).
[5] S. Park, Y. J. Choi, C. L. Zhang, and S.-W. Cheong, Phys. Rev. Lett. **98**, 057601 (2007).
[6] Y. Yamasaki, H. Sagayama, T. Goto, M. Matsuura, K. Hirota, T. Arima, and Y. Tokura, Phys. Rev. Lett. **98**, 147204 (2007).
[7] H. Katsura, N. Nagaosa, and A. V. Balatsky, Phys. Rev. Lett. **95**, 057205 (2005).
[8] C. Jia, S. Onoda, N. Nagaosa, and J. H. Han, Phys. Rev. B **76**, 144424 (2007).
[9] M. Mostovoy, Phys. Rev. Lett. **96**, 067601 (2006).
[10] I. A. Sergienko and E. Dagotto, Phys. Rev. B **73**, 094434 (2006).
[11] H. Murakawa, Y. Onose, K. Ohgushi, S. Ishiwata, and Y. Tokura, J. Phys. Soc. Jpn. **77**, 043709 (2008).
[12] S. Ishiwata, Y. Taguchi, H. Murakawa, Y. Onose, and Y. Tokura, Science **319**, 1643 (2008).
[13] T. Kimura, G. Lawes, and A. P. Ramirez, Phys. Rev. Lett. **94**, 137201 (2005).
[14] N. Momozawa and Y. Yamaguchi, J. Phys. Soc. Jpn. **62**, 1292 (1993).
[15] K. Taniguchi, N. Abe, S. Ohtani, H. Umetsu, and T.-H. Arima, Appl. Phys. Express **1**, 031301 (2008).
[16] Y. Yamasaki, S. Miyasaka, Y. Kaneko, J.-P. He, T. Arima, and Y. Tokura, Phys. Rev. Lett. **96**, 207204 (2006).
[17] N. Momozawa, Y. Nagao, S. Utsumi, M. Abe, and Y. Yamaguchi, J. Phys. Soc. Jpn. **70**, 2724 (2001).
[18] N. Momozawa, Y. Yamaguchi, and M. Mita, J. Phys. Soc. Jpn. **55**, 1350 (1986).
[19] A. Collomb, J. Muller, and T. Fournier, Mater. Res. Bull. **28**, 621 (1993).
[20] J. Smit and H. P. J. Wijn, *Ferrites* (Philips' Technical Library, Eindhoven, The Netherlands, 1959) p. 204.
[21] We assume that the cone angles α and θ are identical for both L and S spins.
[22] A. Malashevich and D. Vanderbilt, Phys. Rev. Lett. **101**, 037210 (2008).
[23] H. J. Xiang, S.-H. Wei, M.-H. Whangbo, and J. L. F. Da Silva, Phys. Rev. Lett. **101**, 037209 (2008).